Specific interactions of ammonium functionalities in amino acids with aqueous fluoride and iodide

Philip E. Mason,[1,*] Jan Heyda, [2] Henry E. Fischer [3], Pavel Jungwirth [2,*]

[1]*Department of Food Science, Cornell University, Ithaca, New York 14853,*
[2]*Institute of Organic Chemistry and Biochemistry, Academy of Sciences of the Czech Republic and Center for Biomolecules and Complex Molecular Systems, Flemingovo nam. 2, 16610 Prague 6, Czech Republic*
[3]*Institut Laue-Langevin, 6 rue Jules Horowitz, BP 156, Grenoble Cedex 9 F-38042, France*

Abstract

Molecular dynamics simulations were performed to examine the relative strength of interactions of fluoride versus iodide with the ammonium (NH_4^+) ion, the alkyl ammonium side chain of lysine ($R_{Lys}NH_3^+$), and the zwitterionic ammonium group of glycine ($R^{(-)}_{Gly}NH_3^+$) in aqueous solution. Clear trends were observed in the ammonium-anion association, with iodide showing essentially constant affinity for all three groups, whereas fluoride interacted most favorably with the ammonium ion, less with $R_{Lys}NH_3^+$, and comparably with iodide with $R^{(-)}_{Gly}NH_3^+$. Neutron scattering experiments show little difference in the interaction of fluoride and iodide with glycine confirming this last observation. The experimental neutron scattering data also suggests that the calculated coordination number of fluoride (about 6 in the constant pressure simulations) is about 20% too high, indicating certain inaccuracies in the classical force field description of this small anion.

[*]*Corresponding authors: pem27@cornell.edu (P.E.M.) and pavel.jungwirth@uochb.cas.cz (P.J.)*

Introduction

The fact that different ions have varying effects on biomolecules in solution has been known for over a hundred years.[1,2] However, over the last few decades the necessity for detailed molecular insight into the origin of these effects, useful for practical applications, combined with a range of methods capable of yielding molecular information about these processes, has led to significant advances in our understanding.[3-7] While there has been a long discussion whether salts alter the stability and/or solubility of proteins primarily via direct interactions, or indirectly by modification of the 'water structure',[8,9] consensus now seems to be growing about the primary importance of the direct mechanism.[4,10-18] Direct interactions are most pronounced with the anionic (glutamic and aspartic acid),[19] cationic amino acids (arginine, lysine and histidine),[10] and the carbonyl oxygen of the backbone peptide bond.[15,20,21]

An empirical Law of matching water affinities,[22,23] stating that oppositely charged ions with matching hydration energies tend to pair in solution, gives us a rough guide for ion specificity in the above interactions. One of the main driving forces behind the present study was to examine the suggestion[24] that the ammonium ion is 'weakly hydrated', therefore by the Law of Matching Water Affinities[22,23] it should interact better with other weakly hydrated ions such as iodide rather than ions such as fluoride. To this end we combined experiment and simulations. Molecular dynamics (MD) has enjoyed a long running, and largely successful partnership with the structural experimental method of neutron scattering.[13,25-29] In order to obtain useful information from neutron scattering data it is necessary to determine an experimental measurement that is sensitive to the critical aspect of the system being examined, which in the current study is the association of halides with the ammonium group of glycine. Given the complexity of the matter in question, the choice of system is explained in greater detail in the data analysis section. Two first order neutron diffraction with isotopic substitution (NDIS)[30,31] difference measurements were conducted on the non-exchangeable hydrogens of glycine, one for glycine in KF and the other in KI. The difference between these measurements is then taken to eliminate all the correlations that are the same in both solutions (namely the intramolecular structure), leaving as a residual the differences in the solvation of glycine in KF and KI solutions.

On the computational side, we examined by MD simulations the interaction of halides with the ammonium moieties of NH_4^+, the alkyl ammonium group of lysine ($R_{Lys}NH_3^+$) and the ammonium group of glycine ($R^{(-)}_{Gly}NH_3^+$) (Figure 1). The relative interactions of fluoride and iodide with $R^{(-)}_{Gly}NH_3^+$ were then compared to neutron scattering measurements on solutions of the same composition.

Simulation details

Molecular dynamics simulations were performed with the aim of studying the distribution of fluoride and iodide in the vicinity of the aqueous ammonium moieties of the ammonium cation, the side chain of terminated lysine, and the zwitterionic form of glycine. The aqueous systems examined were: 3m NH_4F, 3m NH_4I, 2.5m glycine/ 3m KF, 2.5m glycine/ 3m KI and a single terminated (with N-methyl acetamide terminated C-terminus and acylated N-terminus residues) lysine firstly in 3.5 m KF and secondly in 3.5 m KI solution. These systems were examined by both constant volume (NVT), and constant pressure simulations (NpT) with the specific details listed in Table 1. Periodic boundary conditions were applied with cubic box lengths of ~24 – 32 Å (see Table 1 for the exact box sizes and number densities of these systems). Long range electrostatic interactions beyond the non-bonded cutoff of 7.5 - 9.0 Å were accounted for using the Particle Mesh Ewald (PME) method.[32,33] The Berendsen temperature (300 K) and, for constant pressure simulations, pressure (1atm) couplings were employed [34] and all bonds involving hydrogen were constrained using the SHAKE algorithm. [35]

	Glycine NVT	Glycine NpT	Glycine NVT polarizible	Glycine NpT polarizible	Lysine NpT	Ammonium NpT
Number of molecules of anion (F^-, I^-)	36	36	36	36	30	48
Number of counter ion (K^+)	36	36	36	36	29	0
Number of ammonium moieties	30	30	30	30	1	48
Number of water molecules	665	665	665	665	483	886
Box size/ Number density (atoms $Å^{-3}$) **Fluoride**	28.53 0.1020	28.09 0.1067	28.53 0.1020	28.14 0.1062	24.56 0.1041	30.23 0.1066
Box size/ Number density (atoms $Å^{-3}$) **Iodide**	29.43 0.0929	29.58 0.0915	29.43 0.0929	29.55 0.0917	26.31 0.0848	31.52 0.0941

Table 1 Atomic composition and box sizes of the simulated systems. The NVT systems have box sizes based on the experimental densities.

For the polarizable and non-polarizable simulations we used the POL3[36] and SPC/E water models[37] respectively. The polarizable and non-polarizable force fields used for the alkali halides were the same as in our previous studies.[10] For the zwitterionic glycine molecule the parameters were taken from parm99 (which was also used for lysine and ammonium),[38] with charges recalculated at the HF/6-31g* level followed by the RESP procedure. Partial charges for zwitterionic glycine, terminated lysine, and ammonium cation are summarized in the supplementary material Table S1.

All simulations were performed using the AMBER 10 program package.[39] For polarizable simulations, the induced dipoles were converged in each step using a self consistent iteration procedure. A time step of 1 fs was adopted. For each system, minimization and 1ns of equilibration were followed by at least 10 ns of production phase. We checked that such simulation length provided converged results. Trajectories were

primarily analyzed in terms of local concentrations and coordination numbers, based on calculated radial distribution functions between halide anion and the moiety of interest (i.e., ammonium cation, ammonium sidechain group of lysine, or the NH_3^+ terminal group of glycine). This analysis was followed by calculations of ionic spatial probability distributions around interaction sites for halide anions.

Experimental Method

The sample preparation was tailored to the requirements of the neutron diffraction experiment where parity is required between two solutions in all aspects other than the atomic composition of the substituted nuclei, which in this case concerned hydrogenated (*h2*) versus deuterated (*d2*) glycine (Sigma *ReagentPlus* >99 % glycine and Aldrich glycine-2,2-*d2*, 98 atom% D respectively). This involved making stock solutions of KF and KI in D_2O followed by the mixing of correct portions of these solutions and the appropriate amount of glycine. For example, 1.609 g of KF was added to a 25ml pear shaped quickfit flask of known mass and 7ml of D_2O was added. This was then removed on a rotary evaporator such that ~90% of the added D_2O was removed (a D_2O washing to remove most of any light water in the sample). The flask and contents weight was then adjusted by addition of further D_2O to reach the desired concentration of 3 m of salt (for the sake of simplicity here a 3 m solution refers to a ratio of 3 moles of salt to 55.555 of water). To a 5ml nalgene vial was added an accurately weighted mass of glycine (~300mg), and to this was added the exact amount of electrolyte to affect the desired

concentration (~2g) (note in both of the samples used here the exchangeable hydrogens on the glycine were not deuterated).

The prepared solutions were allowed to thermally equilibrate with the reactor temperature for ~2 h before being loaded into a 0.75 ml null scattering Ti/Zr can. Neutron scattering data were collected on the sample for approximately 1 hour. Given the nature of this method, the uncertainty on the parity of the two solutions is essentially limited to the mixing of the glycine and the KF solution, which has estimated errors of ~3 parts per 1000. All data were corrected for multiple scattering and absorption, and normalized versus a vanadium rod using standard procedures.[40] All measurements were performed on the D4C diffractometer at ILL (Grenoble, France)[41] under ambient reactor-hall temperature (23 +/- 0.2 ^{o}C) at a wavelength of 0.7 Å.

Data Analysis

The total measured intensity for the sample (*F(Q)*) is given by

$$F(Q) = \sum_{\alpha} \sum_{\beta} c_{\alpha} c_{\beta} b_{\alpha} b_{\beta} (S_{\alpha\beta}(Q) - 1) \qquad (1)$$

where c_{α} is the atomic concentration of species α, b_{α} is the coherent neutron scattering length, and the sums are over all of the atomic species in solution. $S_{\alpha\beta}(Q)$ is the partial structure factor for atoms α and β. The partial radial distribution function $g_{\alpha\beta}(r)$ is derived from $S_{\alpha\beta}(Q)$ by Fourier transformation:[42]

$$g_{\alpha\beta}(r) = \frac{1}{2\pi^2 \rho r} \int (S_{\alpha\beta}(Q) - 1) \sin(Qr) Q dQ + 1 \qquad (2)$$

The present glycine- KF/KI -water system is complex, since there are 7 types of nuclei: Hex (exchangeable hydrogen atoms on water); O (oxygen on both water and glycine); C (carbon in glycine); N (nitrogen on glycine) and Hnon (the non-exchangeable hydrogen atoms of glycine), potassium, and halide (F^- or I^-). Therefore, F(Q) of this solution is the sum of 28 weighted partial structure factors. In each case the prefactors are numerically expressed as $2c_\alpha c_\beta b_\alpha b_\beta$ (or $c_\alpha c_\beta b_\alpha b_\beta$ when $\alpha = \beta$), where c is the atomic concentration of nuclei of type α and β, and b is the coherent neutron scattering length of that nucleus type.

First order NDIS experiments were conducted on two solutions of glycine of chemically identical composition, one using the naturally abundant *h2* glycine and the other using the sample of *d2* glycine, on the assumption that these two solutions are structurally identical. If a difference is taken between the F(Q)s of these two solution, then all of the correlations exactly cancel out except for those that involve structure factors containing the substituted non-exchangeable hydrogen nuclei. Two first order differences were conducted, *h2*/*d2* substituted glycine (2.5m) in KF (3.0m), and *h2*/*d2* substituted glycine (2.5m) in KI (3.0m). This first order difference function $\Delta S^X_{H_{non}}(Q)$, reduces the twenty eight correlations in the total neutron scattering measurement to seven:

$$\Delta S^{X}_{H_{non}}(Q) = F_{d2-glycine}(Q) - F_{naural-glycine}(Q)$$
$$= A\,[S_{H_{non}H_{ex}}(Q)-1] + B\,[S_{H_{non}O}(Q)-1] + C\,[S_{H_{non}N}(Q)-1] + D\,[S_{H_{non}C}(Q)-1] + E\,[S_{H_{non}H_{non}}(Q)-1]$$
$$+F\,[S_{H_{non}K}(Q)-1] + G\,[S_{H_{non}Y}(Q)-1] \quad (3)$$

The superscript *X* indicates that the function contains only correlations from the substituted nuclei (H_{non}) to all other nuclei in the system. The subscript Y refers to the specific halide in the system, either F^- or I^-. The transform of this function gives the total radial distribution function $\Delta G^{X}_{H_{non}}(r)$,

$$\Delta G^{X}_{H_{non}}(Q) = A\,g_{H_{non}H_{ex}}(r) + B\,g_{H_{non}O}(r) + C\,g_{H_{non}N}(r) + D\,g_{H_{non}C}(r) + E\,g_{H_{non}H_{non}}(r)$$
$$+F\,g_{H_{non}K}(r) + G\,g_{H_{non}Y}(r) - H \quad (4)$$

where H= A+B+C+D+E+F+G and $g_{H_{non}X}(r)$ is the radial distribution function for atoms *X* around the substitution-labeled positions, and A-G are the neutron scattering prefactors for each atom type, which in each case is equal to $2c_{H_{non}}c_X\Delta b_H b_X$ (with the exception of E = $c^2_{H_{non}}\Delta b^2_{H_{non}}$). c_X is the atomic concentration of each atom, b_X is the coherent neutron scattering length of each atom type *X*, and Δb_H is the contrast in the coherent scattering lengths of the substituted nuclei, in this case $\Delta b_H = b_D - b_H$ (deuterium and protium, respectively). The prefactors A-G are provided in Table S2 in the Supporting Information. The solution concentrations (3m of either KF or KI and 2.5m of glycine)

were chosen to yield an experimental measurement that would exemplify the contrast in the behavior of glycine with iodide and fluoride.

It has been found previously that in such measurements, the intermolecular interactions of interest is typically dwarfed by strong intramolecular correlations, and that the non-congruence between the MD and experimental data in the shape of these correlations was such that it rendered direct interpretation of the hydration of the molecule impractical. To bypass these issues the technique of Intramolecular Coordination Number Invariance (ICNCI) was developed.[43] It makes the assumption that the molecular conformation of the substituted molecule does not significantly vary with concentration. Hence, a suitably weighted subtraction of two first order difference would completely remove all molecular correlations and highlight the points of interest, in this case the difference of the solvations of the substituted nuclei of glycine in KF and KI solution. As this technique was developed for rigid solutes with limited flexibility,[43] the question is naturally raised as to if this method is applicable to solutes with higher degrees of freedom. Previous MD studies on glucose, which has both exocyclic hydroxy methyl group, and hydroxyl degrees of freedom found no dependence of these degrees of freedom on concentration over the range 1-5 molal.[31] It is therefore likely that the assumed invariance of molecular conformation with concentration is valid in the present case. From the method described by Mason *et al*,[43] the equivalence of the molecular correlations occurs when

$$\Delta\Delta G^{X}_{H_{non}}(r) = \rho_F G^{X}_{H_{non}}(r)_{Fluoride} - \rho_I G^{X}_{H_{non}}(r)_{Iodide} \ , \qquad (5)$$

where ρ_F and ρ_I are the number densities of the glycine/KF solution and glycine/KI solution respectively.

This may also be expressed in Q space as:

$$\Delta\Delta S^{X}_{H_{non}}(Q) = \Delta S^{X}_{H_{non}}(Q)_{Fluoride} - \Delta S^{X}_{H_{non}}(Q)_{Iodide} \quad (6)$$

where $\Delta\Delta S^{X}_{H_{non}}(Q)$ represents the experimental information that contains no intramolecular correlations; i.e, it contains only intermolecular correlations. While the functions $\Delta\Delta G^{X}_{H_{non}}(r)$ and $\Delta\Delta S^{X}_{H_{non}}(Q)$ carry the same information, they emphasize different parts of it. The function $\Delta\Delta G^{X}_{H_{non}}(r)$ is better for examining the shorter ranges of r and relatively sharp features in real space, while the function $\Delta\Delta S^{X}_{H_{non}}(Q)$ is better at highlighting the longer range structural aspects of the solution which tend to be present in the r space data (if at all) as long range, low amplitude oscillations.

Results

For the MD simulations the density maps of fluoride and iodide around ammonium, the ammonium group of sidechain of lysine ($R_{Lys}NH_3^+$), and glycine ($R^{(-)}_{Gly}NH_3^+$) were evaluated (Figure 2). While all three showed similar patterns, for clarity only the density maps of ammonium and $R^{(-)}_{Gly}NH_3^+$ are shown, as both of these simulations contained 30 ammonium based solutes, versus the single solute in the $R_{Lys}NH_3^+$ simulation. The coordination number of each halide around each species was calculated by integration of the radial distribution function $g_{NHalide}(r)$ up to the first minimum after the first maximum (taken for all calculations as 3.5 and 4.5 Å for the fluoride and iodide simulations respectively (see Table 2 and Supplementary Information, Figure S1) for each of the MD trajectories. Similarly the number of water molecules around the ammonium moieties

was calculated within the same cutoff by integration of the function $g_{NO}(r)$ (Table 2). From the ratio of the number of waters to halides within this cutoff (Table 2) the 'local concentration' was calculated. The effective charge of the ammonium group (the summed charge of the polar nitrogen and hydrogens) and the total effective charge (the effective charge summed with the negative charge of the associated halide) were also calculated (Table 2). The correlations between the effective charge and local concentration and the effective charge and total effective charge were then examined (Figures 3 and 4).

Two analyses were performed on the neutron scattering data (both being variants of the ICNCI technique). The first function (Figure 5) was:

$$\Delta G^{X}_{F-I}(r) = \rho_F G^{X}_{F}(r) - \rho_I G^{X}_{I}(r) \qquad (7)$$

Where ρ_F and ρ_I are the number densities of the *h2* glycine/ KF and *h2* glycine/ KI solutions, and $G^{X}_{F}(r)$ and $G^{X}_{I}(r)$ are the Fourier transforms of the F(Q) of the glycine/ KF and glycine/ KI solutions respectively. This scaled subtraction effectively removes all intramolecular correlations and leaves only differences between the glycine/KF and glycine/KI solution which are primarily the difference in the hydration of the halide.

Similarly, the reciprocal expression of this subtraction was also calculated (Figure 6)

$$\Delta S^{X}_{F-I}(Q) = F^{X}_{F}(Q) - F^{X}_{I}(Q) \qquad (8)$$

The second analysis performed on the neutron scattering data involved the two first order differences of *d2* glycine/ KF and *h2* glycine/ KF ($\Delta S^{X}_{H_{non}}(Q)_{Fluoride}$) and *d2* glycine/

KI and *h2* glycine/ KI ($\Delta S^{X}_{H_{non}}(Q)_{Iodide}$) (Figure 7). An ICNCI type subtraction was performed on these functions (see equation 6) to give the difference function $\Delta\Delta S^{X}_{H_{non}}(Q)$ (Figure 7) in which there are no intramolecular correlations from the substituted nucleus (Hnon) to the glycine. Similarly the real space function $\Delta\Delta G^{X}_{H_{non}}(r)$ (see equation 5) was calculated (Figure 8). For all of the above functions the analogous functions were also evaluated from the NVT molecular dynamics data (Figures 5-10).

ammonium group	Glycine NVT	Glycine NpT	Glycine NVT polarizible	Glycine NpT polarizible	Lysine NpT	Ammonium NpT
Charge on ammonium H	0.295				0.34	0.427
Charge on ammonium N	-0.386				-0.385	-0.707
effective charge of ammonium group	0.499				0.635	1.00
salt	KF	KF	KF	KF	KF	NH_4F
Coordination number of fluoride	0.21	0.19	0.26	0.24	0.53	1.10
Total effective charge	0.29	0.31	0.24	0.26	0.10	-0.10
Coordination number of oxygen	3.65	3.97	3.88	3.70	3.34	5.62
local concentration/ molal	3.21	2.70	3.74	3.59	8.88	10.89
salt	KI	KI	KI	KI	KI	NH_4I
Coordination number of iodide	0.52	0.50	0.44	0.38	0.51	0.59
Total effective charge	-0.02	0.00	0.06	0.12	0.13	0.42
Coordination number of water oxygen	8.01	7.85	8.26	8.15	7.70	9.88
local concentration/ molal	3.58	3.56	2.96	2.60	3.64	3.29

Table 2. Molecular dynamics charges are shown in the upper portion of the table for the polar nitrogen and hydrogens of the ammonium group in question. Lower in black are shown the values calculated from the various MD simulations.

Discussion

In all investigated cases the qualitative form of the interaction of the halide with the ammonium groups is the same (see Figure 2), i.e., a linear NH—Halide hydrogen bond with maximum density for the N...F and N...I contacts occurring at 2.87 and 3.72 Å, respectively. This form is similar to those observed in previous MD studies.[10] However, we find here that the relative strength of interaction of the halides varies considerably with the different ammonium groups in this study. The largest contrast is found between the ammonium cation and the ammonium group of glycine (Figure 2), where in the former case fluoride strongly out competes iodide, whereas for the latter both halides interact comparably with the ammonium group. In this respect, the sidechain ammonium group of lysine lies in-between these two extremes.

While the density map is a direct way of visualizing the variations in relative affinities of iodide and fluoride to different ammonium moieties, there are other methods of characterizing this differential behavior. One of the more useful methods involves calculating the local concentration of halide, which has the advantage of bypassing some of the issues relating to the different cutoffs and ion geometries, being a ratio of ions to water within a certain volume. Here, we found that as the effective charge on the ammonium group increases, so the local concentration of fluoride increases significantly, whereas that of iodide does not (Figure 3). A similar examination of the total effective charge revealed that for fluoride, the higher the effective charge on the ammonium group, the better fluoride is at charge neutralization, eventually 'overcharging' the ammonium ion (Figure 4). However, the opposite trend is observed for iodide, where we found that the lower the charge density of the ammonium group, the more efficient iodide is at

charge neutralization. This leads to an interesting extrapolation; namely, as the charge density decreases and the surface becomes more hydrophobic, iodide should be better than fluoride at negatively charging the surface, which is consistent with previous studies.[24,44,45]

While the general findings of this study are compatible with those from other lines of research, it should be noted that there are certain shortcomings in the fluoride simulations. Notably, while in the NpT simulations the number densities of the iodide simulations are closer to the experimental values (e.g for the 2.5m glycinse/ 3m KI solution: experiment 0.0929 versus MD (NpT) 0.0915 atoms $Å^{-3}$), the fluoride simulations consistently show higher number densities than the experimental values (Table 1). For instance, the difference between the NpT simulated and experimental number densities for the Glycine/ KF solutions was ~4.5% (experiment 0.102 vs MD (NpT) 0.1067 atoms $Å^{-3}$). This discrepancy is arguably symptomatic to fluoride force fields.[46] The majority of the quantum chemistry studies[47-53] suggest the coordination number of F^- is significantly lower than that suggested by classical force field simulations.[54-58] While the majority of simulations to date have focused on a single fluoride ion,[47-53,57-59] there have been several studies performed at finite concentrations. Of these the majority were constant pressure simulations,[54-56,60] while a Reverse-Monte Carlo simulation was performed at constant volume.[61] Typically the MD simulations gave a coordination number of fluoride of ~6,[52,56-59,61] while the quantum calculations typically gave lower values, typically ~5.[48,50,51] This persistent discrepancy can be traced to problems with fluoride force fields. To this end, we made preliminary tests of a new, rationally developed fluoride force field, which provides good match with experimental

solvation free energy and entropy.[46] The pairing of this model of F^- with the ammonium moieties is quantitatively comparable to the results reported here. At the same time, it is encouraging that this new fluoride model has a somewhat lower hydration number and leads to solution densities closer to the experiment.

The obvious suggestion for rationalizing the problems with empirical force fields is that the charge density of the fluoride is high enough to significantly polarize neighboring water molecules. For this reason, we performed simulations of glycine in KF solutions using a polarizable forcefield. While there was a change in the number density in the correct direction, it was rather small (Table 1). This may indicate that the residual problem with fluoride is the partial charge transfer to water, which is difficult to capture accurately with classical force fields.

While the structural measurements performed here were not design to examine fluoride hydration, they do contain information relating to it. The function $\Delta G^X_{F-I}(r)$ is a scaled subtraction of the functions $G^X_F(r)$ and $G^X_I(r)$ such that all the intramolecular correlations that relate to the water or the glycine cancel out exactly. The residual ($\Delta G^X_{F-I}(r)$) contains only components that relate to the difference in the solution structure due to the difference in the hydration of the respective halides. This can be directly shown by the examination of these functions calculated from the molecular dynamics data (Figure 9). Further the contribution of individual radial pair distribution functions to this difference function can be examined in the data calculated from the MD simulations. This analysis reveals that the majority of the contribution to the first peak at 1.6 Å is due to the F-H correlation (which has no counterpart in the potassium iodide solution, Figure 10). This function can also be calculated from the neutron scattering

data. Assuming that the whole of the first peak is due to the F-H correlation (with the hydrogens in this case being both the exchangeable hydrogens on glycine and water) then this peak can be integrated to yield a coordination number. We found that the coordination number of fluoride was somewhat lower than the molecular dynamics predicts, i.e., about 5 for the experiment, and 6 for the MD simulation (Figure 9). While this integral is not numerically meaningful after the first peak, as the assumption that this is only due to the F-H correlation breaks down, it is nonetheless indicative of the difference of hydration of fluoride between simulations and experiments. Again it is generally found that the rolling coordination number for the MD simulation is about 20% higher than that of the experiment. This metric, combined with the difference in the number density between the constant pressure simulation and the experiment suggest that fluoride coordination is indeed somewhat too high in the MD simulations.

Nevertheless, the prime goal of the experiment in this study was to examine the difference in the association of different ammonium moieties with either fluoride or iodide. Initially, we planned to use ammonium fluoride and iodide. Unfortunately in 3 m NH_4F solution, the concentration of free HF is so high that it almost immediately attacks the Ti/Zr alloy from which the neutron scattering cell was made. Luckily, we found that solutions of the zwitterionic glycine and potassium fluoride were passive towards Ti/Zr. Thus, given the relatively high solubility of glycine (~3 m at 20 ^{o}C in H_2O) we decided to use it as a first proxy for the ammonium group, only to find later with the help of simulations that it exhibits very different relative affinities to fluoride and iodide.

The normalized total scattering functions $F(Q)$ for all four solutions (H/D substituted glycine in KF and KI) and the first order difference functions ($\Delta S^{X}_{H_{non}}(Q)$) are

shown in figure 7. The second order difference function $\Delta\Delta S^{X}_{H_{non}}(Q)$ is also shown for both the NVT MD simulation and the measurement. These results suggest very small differences in the solvation of the non exchangeable hydrogens of glycine (which are present right next to the zwitterionic ammonium group) between 3m KF and 3m KI. While the fit of MD to the experiment is only semiquantitative, the key feature that seems to be born out from both approaches is that the difference between solvation of glycine in KF *vs* KI solution is small. As previous studies have been able to differentiate between strong and weak counter-ion association in comparative studies of $CsNO_3$ and Cs_2CO_3,[28] and GdmSCN and Gdm_2SO_4,[13] it seems reasonable that the 'null' result obtained here is genuine. Further from the MD simulations we make the prediction that if a suitable measurement can be made to examine the difference in the ion pairing between NH_4F *vs* NH_4I that a significant contrast (i.e., more favorable pairing for fluoride) should be found, as compared to the present measurements of glycine.

Conclusions

A significant trend was found from MD simulations that the relative strengths of association of fluoride vs iodide with a series of ammonium moieties (NH_4^+, $R_{Lys}NH_3^+$ and $R^{(-)}_{Gly}NH_3^+$) varies with the effective charge of the ammonium group. In the case of glycine- F^- and I^- association, the relative strengths of interactions from the MD studies was supported by neutron scattering experiments. Fluoride showed the highest affinity for the group with highest charge density, i.e., NH_4^+, while the local concentration of iodide was not greatly affected by the effective charge of a given the ammonium moiety. As the effective charge decreases, fluoride thus becomes less effective at charge

neutralization of the ammonium group, while an opposite (and weaker) trend was observed for iodide. As a result there is a crossover – F^- is more attracted to NH_4^+ and $R_{Lys}NH_3^+$ than I^-, but less to $R^{(-)}_{Gly}NH_3^+$. We also found that the neutron scattering measurements indicated that the coordination number of fluoride given by MD simulations (i.e., ~6) is somewhat too high, and that a coordination number of ~5, as suggested by quantum mechanical studies is more realistic.

Acknowledgment

Support from the Czech Science Foundation (grant 203/08/0114) and the Czech Ministry of Education (grant LC512) is gratefully acknowledged. J. H. thanks the International Max-Planck Research School for support. Part of the work in Prague was supported via Project Z40550506.

Figure captions:

Figure 1. The ammonium groups in this study, from left to right, NH_4^+, middle, $R_{Lys}NH_3^+$ and right $R_{Gly}NH_3^+$ along with the size of the fluoride and iodide ion (green and purple respectively).

Figure 2. The density maps around the ammonium group (right) and the ammonium group of glycine (left) of fluoride (green) and iodide (purple) as calculated from the NpT simulations. In all cases the contour level is the same at 10.7x the bulk number density of that ion. The density map of $R_{Lys}NH_3^+$ is not shown as this simulation only contained one solute, while the NH_4^+ and $R_{Gly}NH_3^+$ simulations both contained 30 solute.

Figure 3. The local concentration of halide next to the ammonium group as calculated from the NpT simulations (green fluoride, purple iodide). In each case the lowest effective charge point is for the ammonium group of glycine, the middle point for the sidechain ammonium group of lysine and the right point the ammonium ion.

Figure 4. The total effective charge (the effective charge of the ammonium group plus the charge of the associated halide), versus the effective charge of the ammonium group as calculated from the NpT simulations (green fluoride, purple iodide). In each case the lowest effective charge point is for the ammonium group of glycine, the middle point for the sidechain ammonium group of lysine and the right point the ammonium ion.

Figure 5. Lower black is shown the raw functions $\Delta G^X_{F-I}(r)$, and when the difference is calculated after the HO correlation in the totals (the fourier transform of F(Q)), which is the cause of much of the ringing, has been removed by fourier filtering (red).[28] Upper red is shown the same experimental measurement in comparison to that calculated from the NVT simulations (blue). The NVT data is used here such that both the experimental and simulated densities are identical. This is preferred for the ICNCI comparison as otherwise there is a baseline shift corresponding to the different densities of the NpT simulation and experimental data.

Figure 6. The raw reciprocal space difference function $\Delta S^X_{F-I}(Q)$ (lower black). The slight slope is due to the somewhat different placzek effect between the two solution. Upper is shown the comparison between the MD prediction for $\Delta S^X_{F-I}(Q)$ (from the

NVT simulations, grey) versus that from the experiment after the removal of the placzek background.[28,62]

Figure 7. The application of the ICNCI method. Upper left and right are shown the total scattering measurement (F(Q) for KF/glycine and KI/glycine respectively. In each case the black and grey line correspond to the *h2* and *d2* substituted glycine respectively. Lower left are shown the first order difference functions, grey for the KF/ glycine solution, black for the KI/glycine solution. Lower right is shown the ICNCI function $\Delta\Delta S^{X}_{H_{non}}(Q)$ from the experiment (grey) versus the calculation of this function from the molecular dynamics (black).

Figure 8. The function $\Delta\Delta G^{X}_{H_{non}}(r)$ as calculated directly from the NVT MD calculations (black) and from the experimental data (grey).

Figure 9. Experimental data (same as in Figure 5) are shown in red, while the MD results are depicted in black. The faded data and right scale corresponds to the function $\Delta G^{X}_{F-I}(r)$ (the peak at ~1.7 Å is due to the F-H correlation), while the left scale and bold lines are the coordination numbers calculated on the assumption that this portion of the function is solely due to the H-F correlation.

Figure 10. Using the MD predictions of the experimental measurement to demonstrate the technique used for extracting information of the fluoride hydration from the neutron scattering data. a) the predicted total real space functions (G(r)) for the KF/glycine solution (black) and KI/glycine solution (red). Lower is shown the function $\Delta G^{X}_{F-I}(r)$ calculated by the scaled subtraction of the upper two plots. In blue is shown the component of this function that is due to the difference of the H-F and H-I correlations. The peak at 1.7 is almost solely due to the H-F correlation due to the hydration of the fluoride ion that does not occur in the KI/glycine solution.

Figure 1

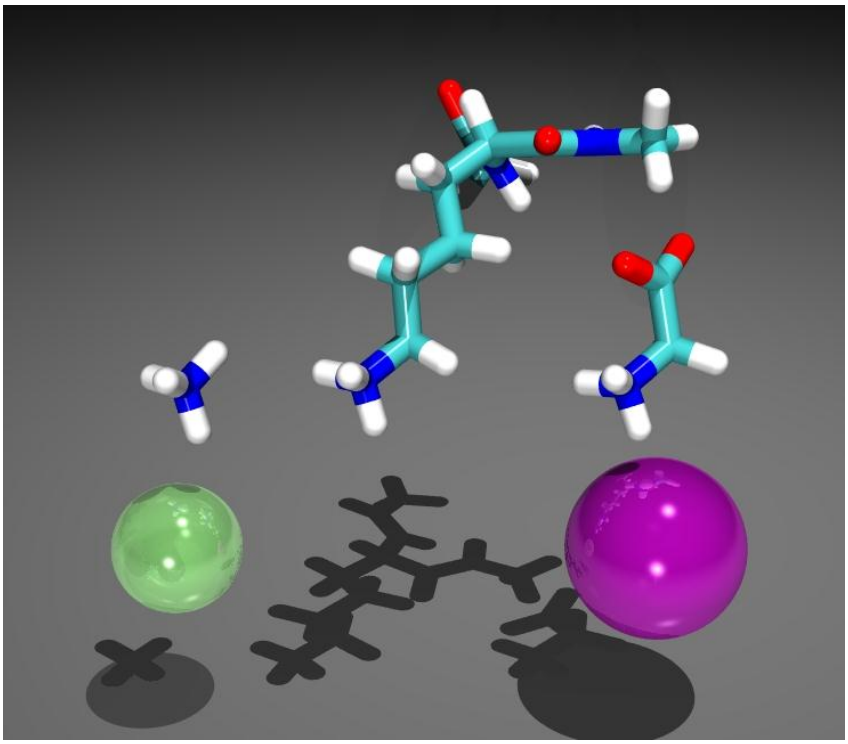

Figure 2

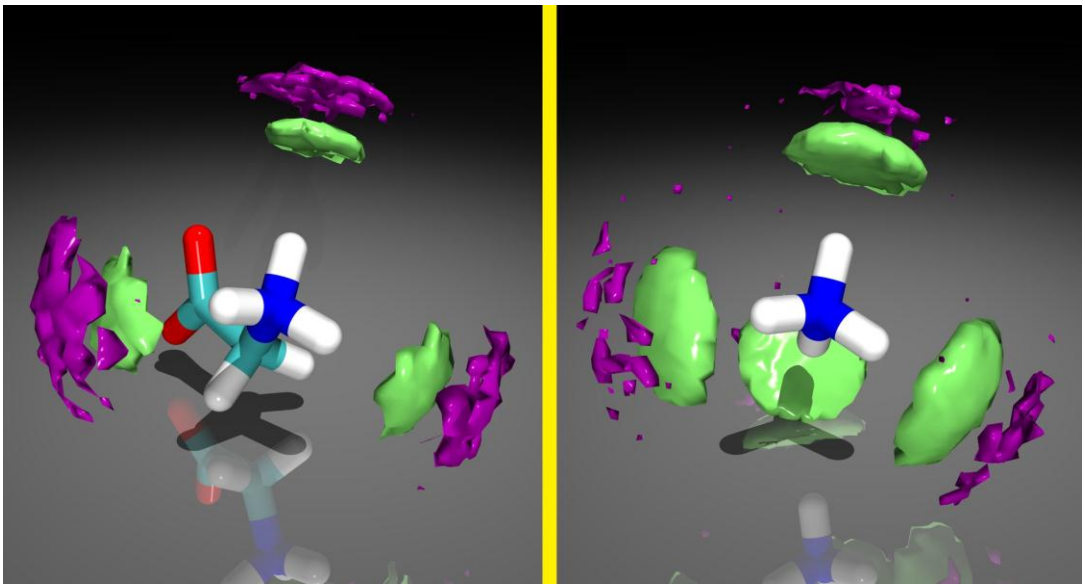

Figure 3

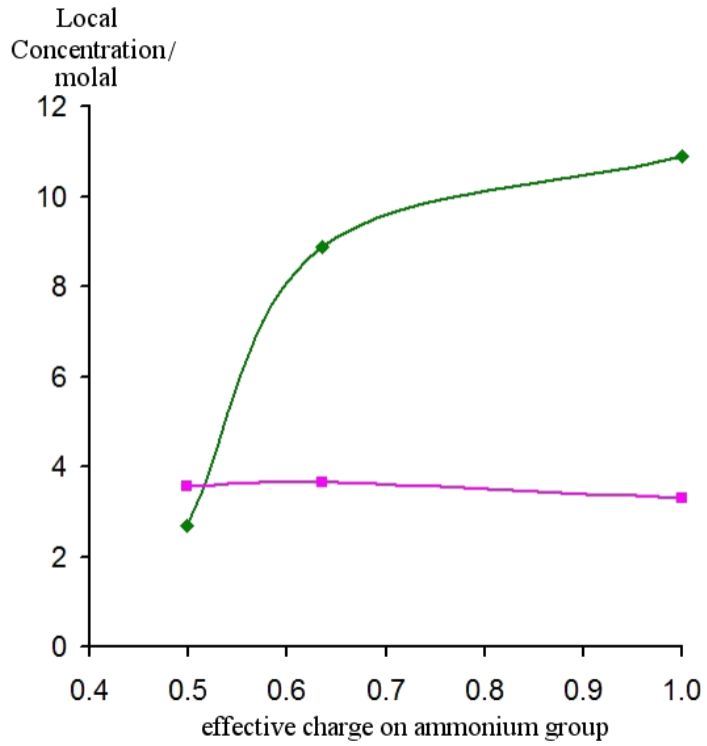
Local
Concentration/
molal
12
10
8
6
4
2
0
0.4
0.5
0.6
0.7
0.8
0.9
1.0
effective charge on ammonium group

Figure 4

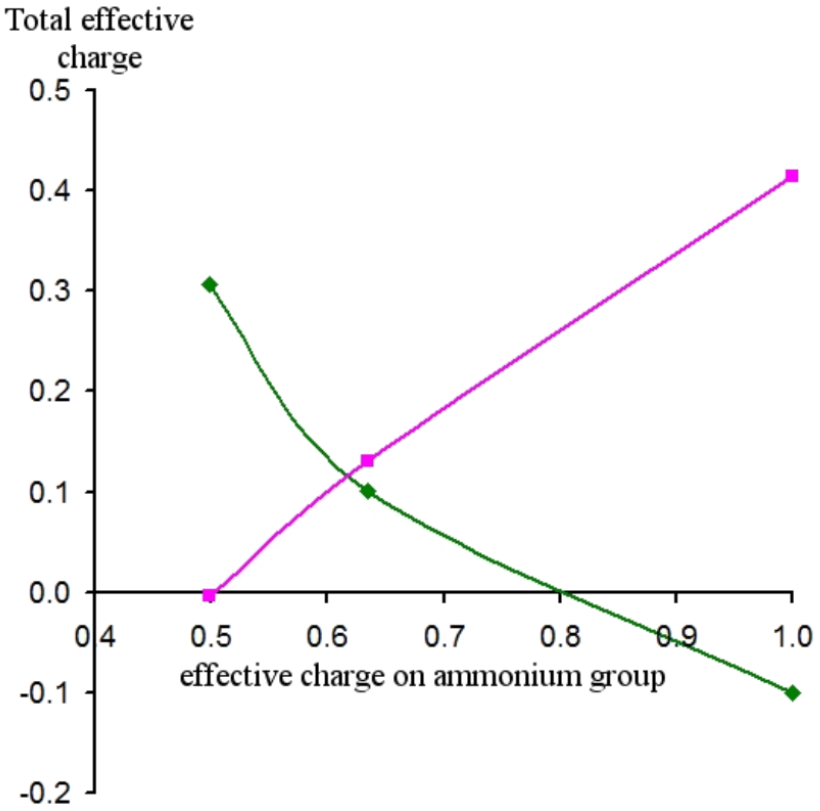
Total effective charge
0.5
0.4
0.3
0.2
0.1
0.0
-0.1
-0.2
0.4
0.5
0.6
0.7
0.8
0.9
1.0
effective charge on ammonium group

Figure 5

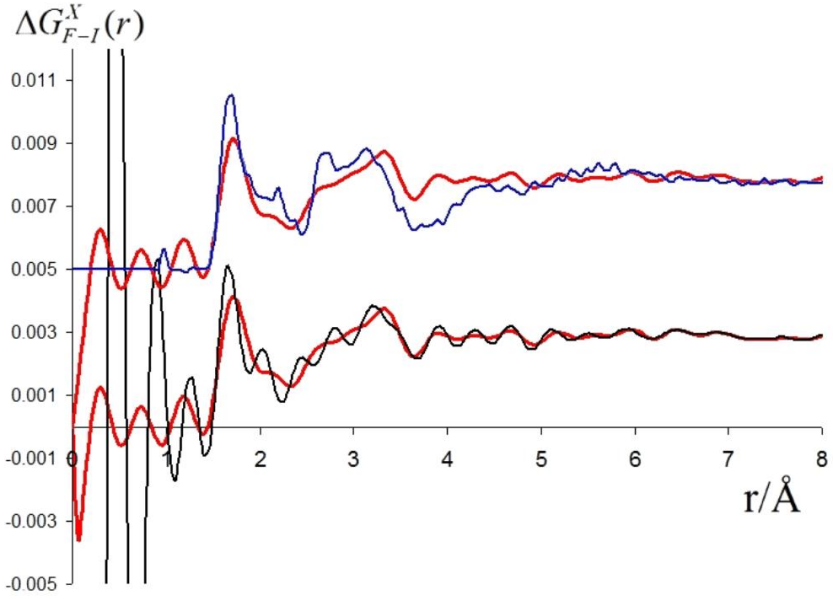
$\Delta G^{X}_{F-I}(r)$
0.011
0.009
0.007
0.005
0.003
0.001
-0.001
-0.003
-0.005
0
1
2
3
4
5
6
7
8
r/Å

Figure 6

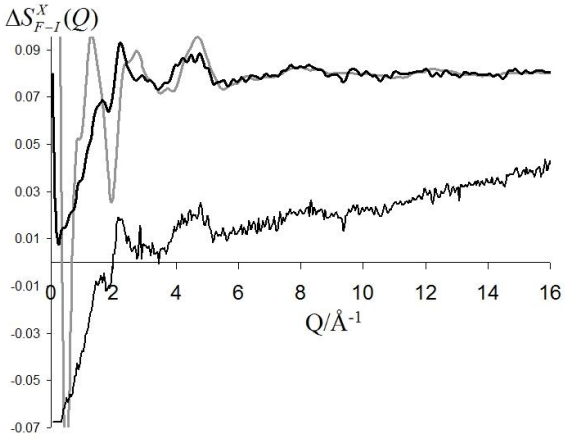
$\Delta S^{X}_{F-I}(Q)$
0.09
0.07
0.05
0.03
0.01
-0.01
-0.03
-0.05
-0.07
0
2
4
6
8
10
12
14
16
Q/Å^{-1}

Figure 7

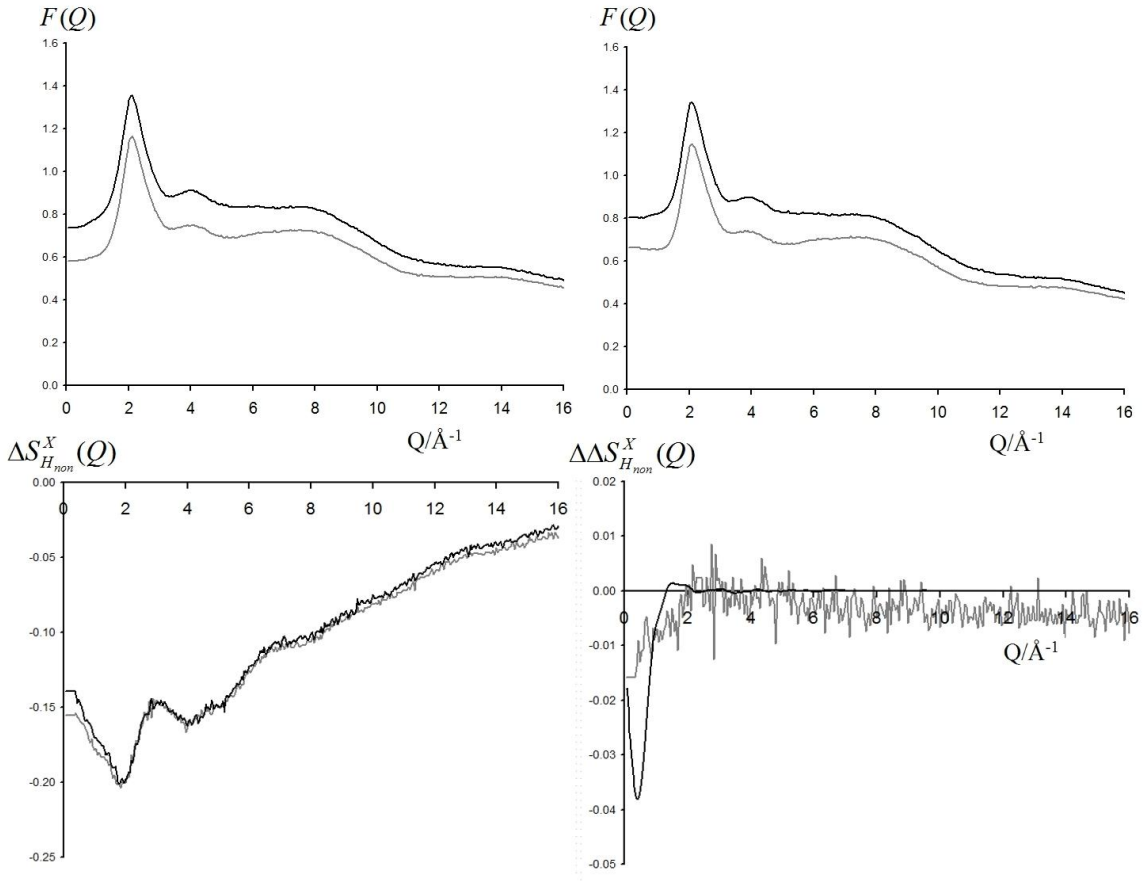

Figure 8

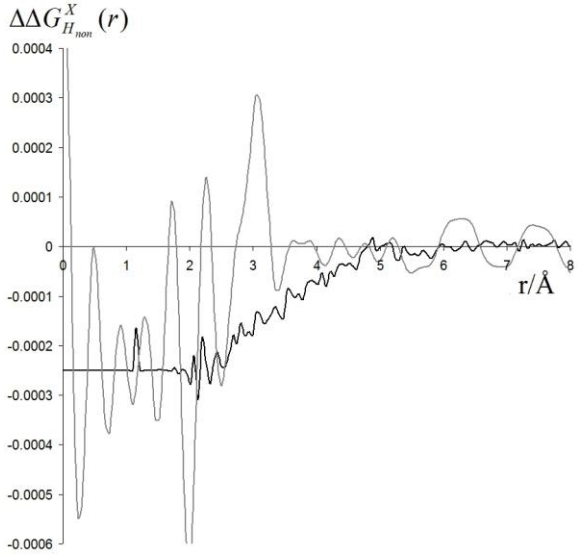
$\Delta\Delta G^{X}_{H_{non}}(r)$
0.0004
0.0003
0.0002
0.0001
0
-0.0001
-0.0002
-0.0003
-0.0004
-0.0005
-0.0006
0
1
2
3
4
5
6
7
8
r/Å

Figure 9

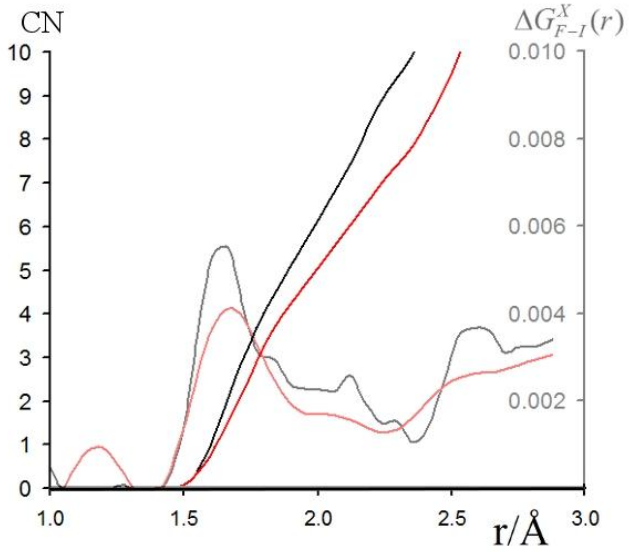
CN
$\Delta G^{X}_{F-I}(r)$
10
9
8
7
6
5
4
3
2
1
0
0.010
0.008
0.006
0.004
0.002
1.0
1.5
2.0
2.5
3.0
r/Å

Figure 10

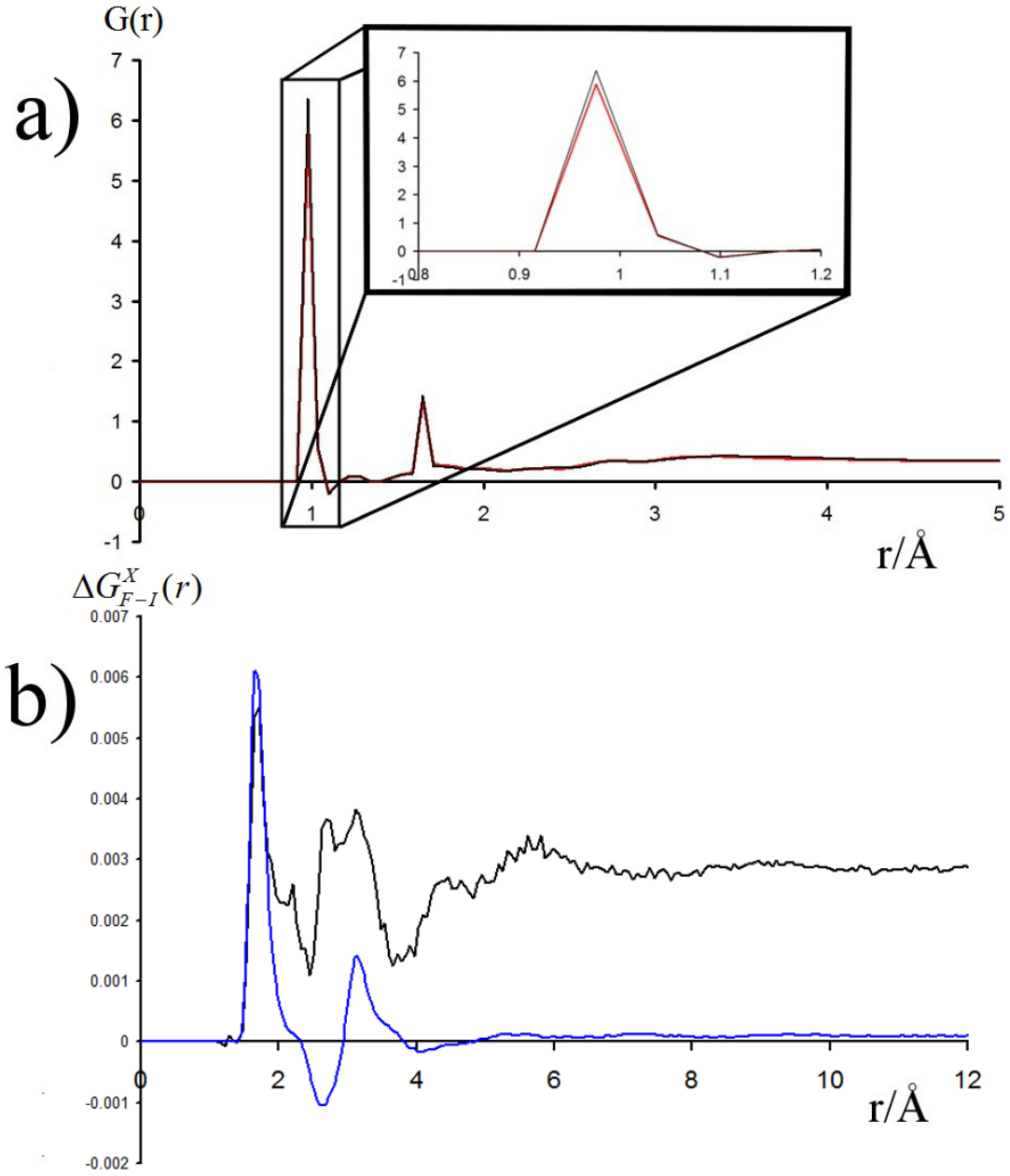

References

(1) Hofmeister, F. **Zur** Lehre von der Wirkung der Salze *Archiv für Experimentel*le Pathologie und Pharmakologie, 1888; Vol. 24; pp 247.

(2) Kunz, W.; Henle, J.; Ninham, B. W. *Current Opinion in Colloid & Interface Science* **2004**, *9*, 19.

(3) Kunz, W. *Current Opinion in Colloid & Interface Science* **2010**, *15*, 34.

(4) Zhang, Y. J.; Furyk, S.; Bergbreiter, D. E.; Cremer, P. S. *Journal of the American Chemical Society* **2005**, *127*, 14505.

(5) Collins, K. D.; Neilson, G. W.; Enderby, J. E. *Biophysical Chemistry* **2007**, *128*, 95.

(6) Rydall, J. R.; Macdonald, P. M. *Biochemistry* **1992**, *31*, 1092.

(7) Cheng, J.; Vecitis, C. D.; Hoffmann, M. R.; Colussi, A. J. *Journal of Physical Chemistry B* **2006**, *110*, 25598.

(8) Dixit, S.; Soper, A. K.; Finney, J. L.; Crain, J. *Europhysics Letters* **2002**, *59*, 377.

(9) Scott, J. N.; Nucci, N. V.; Vanderkooi, J. M. *Journal of Physical Chemistry A* **2008**, *112*, 10939.

(10) Heyda, J.; Hrobarik, T.; Jungwirth, P. *Journal of Physical Chemistry A* **2009**, *113*, 1969.

(11) Dempsey, C. E.; Piggot, T. J.; Mason, P. E. *Biochemistry* **2005**, *44*, 775.

(12) Dempsey, C. E.; Mason, P. E.; Bracly, J. W.; Neilson, G. W. *Journal of the American Chemical Society* **2007**, *129*, 15895.

(13) Mason, P. E.; Dempsey, C. E.; Neilson, G. W.; Brady, J. W. *Journal of Physical Chemistry B* **2005**, *109*, 24185.

(14) Mason, P. E.; Brady, J. W.; Neilson, G. W.; Dempsey, C. E. *Biophysical Journal* **2007**, *93*, L4.

(15) Heyda, J.; Vincent, J. C.; Tobias, D. J.; Dzubiella, J.; Jungwirth, P. *Journal of Physical Chemistry B* **2010**, *114*, 1213.

(16) Mason, P. E.; Dempsey, C. E.; Vrbka, L.; Heyda, J.; Brady, J. W.; Jungwirth, P. *Journal of Physical Chemistry B* **2009**, *113*, 3227.

(17) Vondrasek, J.; Mason, P. E.; Heyda, J.; Collins, K. D.; Jungwirth, P. *Journal of Physical Chemistry B* **2009**, *113*, 9041.

(18) Pegram, L. M.; Record, M. T. *Journal of Physical Chemistry B* **2008**, *112*, 9428.

(19) Heyda, J.; Pokorna, J.; Vrbka, L.; Vacha, R.; Jagoda-Cwiklik, B.; Konvalinka, J.; Jungwirth, P.; Vondrasek, J. *Physical Chemistry Chemical Physics* **2009**, *11*, 7599.

(20) Auton, M.; Holthauzen, L. M. F.; Bolen, D. W. *Proceedings of the National Academy of Sciences of the United States of America* **2007**, *104*, 15317.

(21) Street, T. O.; Bolen, D. W.; Rose, G. D. *Proceedings of the National Academy of Sciences of the United States of America* **2006**, *103*, 13997.

(22) Collins, K. D. *Proceedings of the National Academy of Sciences of the United States of America* **1995**, *92*, 5553.

(23) Collins, K. D. *Biophysical Journal* **1997**, *72*, 65.

(24) Collins, K. D. *Biophysical Chemistry* **2006**, *119*, 271.

(25) Bowron, D. T.; Soper, A. K.; Finney, J. L. *Journal of Chemical Physics* **2001**, *114*, 6203.

(26) Soper, A. K. *Molecular Physics* **2001**, *99*, 1503.

(27) Yamaguchi, T.; Hidaka, K.; Soper, A. K. *Molecular Physics* **1999**, *96*, 1159.

(28) Mason, P. E.; Neilson, G. W.; Dempsey, C. E.; Brady, J. W. *Journal of the American Chemical Society* **2006**, *128*, 15136.

(29) Mason, P. E.; Dempsey, C. E.; Neilson, G. W.; Kline, S. R.; Brady, J. W. *Journal of the American Chemical Society* **2009**, *131*, 16689.

(30) Neilson, G. W.; Enderby, J. E. *Proceedings of the Royal Society of London Series a-Mathematical Physical and Engineering Sciences* **1983**, *390*, 353.

(31) Mason, P. E.; Neilson, G. W.; Barnes, A. C.; Enderby, J. E.; Brady, J. W.; Saboungi, M. L. *Journal of Chemical Physics* **2003**, *119*, 3347.

(32) Darden, T.; York, D.; Pedersen, L. *Journal of Chemical Physics* **1993**, *98*, 10089.

(33) Essmann, U.; Perera, L.; Berkowitz, M. L.; Darden, T.; Lee, H.; Pedersen, L. G. *Journal of Chemical Physics* **1995**, *103*, 8577.

(34) Berendsen, H. J. C.; Postma, J. P. M.; Vangunsteren, W. F.; Dinola, A.; Haak, J. R. *Journal of Chemical Physics* **1984**, *81*, 3684.

(35) Ryckaert, J. P.; Ciccotti, G.; Berendsen, H. J. C. *Journal of Computational Physics* **1977**, *23*, 327.

(36) Caldwell, J. W.; Kollman, P. A. *J. Phys. Chem.* **1995**, *99*, 6208.

(37) Berendsen, H. J. C.; Grigera, J. R.; Straatsma, T. P. *Journal of Physical Chemistry* **1987**, *91*, 6269.

(38) Wang, J. M.; Wolf, R. M.; Caldwell, J. W.; Kollman, P. A.; Case, D. A. *Journal of Computational Chemistry* **2004**, *25*, 1157.

(39) Case, D. A.; Darden, T. A.; Cheatham, T. E., III.; Simmerling, C. L.; Wang, J.; Duke, R. E.; Luo, R.; Crowley, M. R. C. W.; Zhang, W.; Merz, K. M.; Wang, B.; Hayik, S.; Roitberg, A.; Seabra, G.; Kolossvary, I. K. F. W.; Paesani, F.; Vanicek, J.; Wu, X.; Brozell, S. R.; Steinbrecher, T.; Gohlke, H.; Yang, L. C. T.; Mongan, J.; Hornak, V.; Cui, G.; Mathews, D. H.; Seetin, M. G.; Sagui, C.; Babin, V.; Kollman, P. A. Amber 10; University of California, San Francisco: San Francisco, 2008.

(40) Barnes, A. C.; Enderby, J. E.; Breen, J.; Leyte, J. C. *Chemical Physics Letters* **1987**, *142*, 405.

(41) Fischer, H. E.; Cuello, G. J.; Palleau, P.; Feltin, D.; Barnes, A. C.; Badyal, Y. S.; Simonson, J. M. *Applied Physics a-Materials Science & Processing* **2002**, *74*, S160.

(42) Soper, A. K.; Neilson, G. W.; Enderby, J. E.; Howe, R. A. *Journal of Physics C-Solid State Physics* **1977**, *10*, 1793.

(43) Mason, P. E.; Neilson, G. W.; Dempsey, C. E.; Price, D. L.; Saboungi, M. L.; Brady, J. W. *Journal of Physical Chemistry B* **2010**, *114*, 5412.
(44) Lund, M.; Jungwirth, P. *Journal of Physics-Condensed Matter* **2008**, *20*.
(45) Lund, M.; Vacha, R.; Jungwirth, P. *Langmuir* **2008**, *24*, 3387.
(46) Horinek, D.; Mamatkulov, S. I.; Netz, R. R. *Journal of Chemical Physics* **2009**, *130*, 21.
(47) Joung, I. S.; Cheatham, T. E. *Journal of Physical Chemistry B* **2008**, *112*, 9020.
(48) Ohrn, A.; Karlstrom, G. *Journal of Physical Chemistry B* **2004**, *108*, 8452.
(49) Craig, J. D. C.; Brooker, M. H. *Journal of Solution Chemistry* **2000**, *29*, 879.
(50) Ho, M. H.; Klein, M. L.; Kuo, I. F. W. *Journal of Physical Chemistry A* **2009**, *113*, 2070.
(51) Heuft, J. M.; Meijer, E. J. *Journal of Chemical Physics* **2005**, *122*, 7.
(52) Jensen, K. P.; Jorgensen, W. L. *Journal of Chemical Theory and Computation* **2006**, *2*, 1499.
(53) Zhan, C. G.; Dixon, D. A. *Journal of Physical Chemistry A* **2004**, *108*, 2020.
(54) Sanz, E.; Vega, C. *Journal of Chemical Physics* **2007**, *126*, 13.
(55) dos Santos, D.; Muller-Plathe, F.; Weiss, V. C. *Journal of Physical Chemistry C* **2008**, *112*, 19431.
(56) Laudernet, Y.; Cartailler, T.; Turq, P.; Ferrario, M. *Journal of Physical Chemistry B* **2003**, *107*, 2354.
(57) Koneshan, S.; Rasaiah, J. C.; Lynden-Bell, R. M.; Lee, S. H. *Journal of Physical Chemistry B* **1998**, *102*, 4193.
(58) Lee, S. H.; Rasaiah, J. C. *Journal of Physical Chemistry* **1996**, *100*, 1420.
(59) Lamoureux, G.; Roux, B. *Journal of Physical Chemistry B* **2006**, *110*, 3308.
(60) Ferrario, M.; Ciccotti, G.; Spohr, E.; Cartailler, T.; Turq, P. *Journal of Chemical Physics* **2002**, *117*, 4947.
(61) Soper, A. K.; Weckstrom, K. *Biophysical Chemistry* **2006**, *124*, 180.
(62) Mason, P. E.; Neilson, G. W.; Enderby, J. E.; Saboungi, M. L.; Brady, J. W. *Journal of Physical Chemistry B* **2005**, *109*, 13104.

TOC Figure